Separation and Purification Technology 264 (2021) 118430

Contents lists available at ScienceDirect

Separation and Purification Technology

journal homepage: www.elsevier.com/locate/seppur

Single-step synthesis of a polyelectrolyte complex hollow-fiber membrane for forward osmosis

M. Mohammadifakhr [a], J. de Grooth [a,c], K. Trzaskus [b], H.D.W. Roesink [a], A.J.B. Kemperman [a,*]

[a] Membrane Science and Technology, Faculty of Science and Technology, Mesa+ Institute for Nanotechnology, University of Twente, P.O. Box 217, 7500 AE Enschede, the Netherlands
[b] Department of Research and Development, Aquaporin A/S, Nymøllevej 78, 2800 Kongens Lyngby, Denmark
[c] Films in Fluids, Faculty of Science and Technology, Mesa+ Institute for Nanotechnology, University of Twente, P.O. Box 217, 7500 AE Enschede, the Netherlands

ARTICLE INFO

Keywords:
Forward osmosis
Hollow-fiber membranes
Polyelectrolyte complex
Selective layer deposition
PSS
PDADMAC

ABSTRACT

We present the simultaneous synthesis of a hollow fiber membrane with a selective layer created by means of polyelectrolyte complexation (PEC), to be used as a membrane in forward osmosis. The aim of this single-step approach was to create a defect-free robust selective layer and circumvent the challenges associated with coating via interfacial polymerization. The nascent hollow fiber membrane with a PEC layer was characterized by SEM imaging as well by determining the streaming potential and pure water permeance. We also evaluated several electrolytes as potential draw solutes in combination with the developed membrane and selected trisodium citrate (TSC) as it showed a very high rejection of 97 ± 2%. Using 1 M TSC as draw solution showed promising osmotic performance in selective layer facing feed solution (FO) mode, having a water flux of 7.8 ± 0.2 ($L \cdot m^{-2} \cdot h^{-1}$) and a reverse salt flux of 2.1 ± 0.7 ($g \cdot m^{-2} \cdot h^{-1}$). A significantly higher reverse salt flux of was gained in PRO mode which was attributed to the high ionic strength of the charged draw solute near the PEC layer. It is highlighted that the choice of draw solute as well as process orientation (FO or PRO mode) are crucial for charged selective layers such as our PEC selective layer. We conclude that our approach shows substantial promise for use in FO processes using TSC as the draw solution. In addition, the taken approach successfully eliminates the time-consuming and challenging extra step of coating hollow fibers through interfacial polymerization, opening up opportunities for the cost-effective synthesis of FO hollow-fiber membranes.

1. Introduction

The forward osmosis (FO) principle benefits from the movement of water from a dilute solution (feed) towards a concentrate solution (draw) based on the osmotic pressure gradient [1]. Forward osmosis (FO) can be used in various applications such as seawater desalination [2], food processing [3–5], and wastewater treatment [6]. One of the advantages of FO is the usage of waste or low-quality energy (e.g., high saline brine or residual heat) instead of clean energy (electricity). A major obstacle for FO membranes is the internal concentration polarization (ICP) occurring inside the support. This is due to the support showing resistance toward mass transport leading to a lower osmotic pressure (driving force) [7]. The severity of ICP is affected by several parameters such as support properties [8], the orientation of the FO process [9] and the draw solution [10]. Another challenge is the reverse salt flux which is basically the diffusion of the draw solutes into the feed solution, which needs to be as low as possible. Typically a highly concentrated draw solution is used (>0.5 M) in order to have a reasonable osmotic water flux [11]. However, this high concentration increases the chance of the draw's solute passage to feed solution [12] which is highly unfavorable. The reversed salt flux leads to a reduction in driving force and consequently a drop in the osmotic water flux [12–14]. Therefore, a highly selective layer is essential for FO membranes which ensures both a low salt flux as well as a high osmotic flux [15]. In addition, the choice of draw solutes is crucial, especially for polyelectrolyte-based membranes where the charge of the solute influences the rejection of the selective layer [16].

Currently, thin-film composite membranes prepared by interfacial polymerization (IP) are the most common membranes used in FO processes [17–20]. However, the IP procedure is a sensitive and challenging method with low reproducibility. This is because of its stringent dependence on various parameters such as experimental conditions,

* Corresponding author.
E-mail address: a.j.b.kemperman@utwente.nl (A.J.B. Kemperman).

https://doi.org/10.1016/j.seppur.2021.118430
Received 9 October 2020; Received in revised form 29 January 2021; Accepted 30 January 2021
Available online 7 February 2021

choice of monomers, and the support's surface properties [21,22]. A major issue associated with selective layer formation via IP is a lack of attachment to the support [23], which can happen for both flat sheets and hollow fibers. Delamination occurs if the selective layer does not penetrate sufficiently into the support's surface pores [24]. A second obstacle is related to the monomers used in the IP reaction, commonly m-phenylenediamine (MPD) and trimesoyl chloride (TMC). For example, an excess amount of MPD on the support leads to defects in the selective (polyamide) layer as the excess MPD prevents the reaction from happening at the surface of the support, resulting in pin holes [25]. Excess MPD can be easily removed from flat sheets by using a rubber roller. With hollow fibers, removal typically is done by purging the excess MPD from the lumen side with a gas stream. If this gas purge is not long enough, droplets of the MPD solution may remain on the support's surface; on the other hand, a very long gas purge may lead to drying out of the MPD solution [25]. Consequently, hollow fibers are more prone to defects in the selective layer on their inner surface than flat sheets. Moreover, flowing of the MPD or TMC solutions in the bore of the fiber leads to a pressure drop along the length of the membrane, which results in differences in the distribution of monomers near the surface.

Although hollow fiber supports are more difficult to coat on the inner side, they have several inherent advantages over spiral wound (flat-sheet) membranes. Firstly, hollow fiber membranes have a much larger surface area per unit volume, which results in a higher productivity per unit volume of a membrane module [26]. In addition, as these modules are spacer-free, hollow fibers offer the advantages of low fouling tendencies and easy cleaning [27]. Moreover, the flexibility in tuning the inner diameter of fibers makes them highly suitable for treating highly viscous solutions.

To be able to benefit from the advantages of hollow fibers, a better preparation method for the selective layer is needed. One alternative is the use of a polyelectrolyte Layer-by-Layer (LbL) assembly, which results in polyelectrolyte multilayer membranes (PEMMs). The LbL assembly method has proven successful for hollow fibers [28] and the use of PEMMs in FO has recently been studied [29–33]. PEMMs are prepared by the alternating adsorption of two oppositely charged polyelectrolytes on porous supports [34]. One advantage of thin-film formation by polyelectrolytes is the usage of water as solvent, which makes the whole process more environmentally sustainable. A second advantage is that this versatile and simple technique results in more control over the final thickness of the selective layer [35]. On the other hand, for the fabrication of the PEMMs, multiple layers have to be deposited onto the inner surface of a fiber to achieve sufficient rejection [35]; this is time-consuming and might be expensive on an industrial scale. The second disadvantage is that PEMMs are not highly selective towards the commonly used NaCl draw solution. To the best of our knowledge, only one polyelectrolyte multilayer-based membrane has been reported in the literature so far that was prepared with this technique that showed a high rejection of small charged solutes (Na^+, Cl^-), but only after chemical modification of the LbL layer [36].

Hence, different draw solutions could be favorable when polyelectrolyte multilayer based selective layers are used to avoid a high reverse salt flux. These alternative draw solutions with larger hydrated radii include charged draw solutions such as $MgCl_2$ [37,38], Na_2SO_4 [39], $MgSO_4$ [40,41] and trisodium citrate (TSC) [42,43] and uncharged solutions such as sucrose [43,44] and glucose [40,41,43,45]. Specifically, for polyelectrolyte-based membranes one important property of the draw solution that must be considered is the charge of the solutes. Charged draw solutes influence the rejection of the polyelectrolyte-based selective layer and thus the reverse salt flux. This is because charged draw solutes can result in swelling of the polyelectrolyte layer and reduced charged-based solute exclusion [46], especially under high ionic strengths like with the draw solutions used in FO. Both result in lower rejection of the polyelectrolyte (PE)-based selective layer as well as higher reverse salt flux. In addition, Donnan dialysis is phenomenon that can occur when using charged draw solutes and leads to counter diffusion of two or more ions as well as the electrostatic interactions which would result in draw ions attracting the oppositely charged feed ions towards the draw solution side [47]. Both phenomena lead to movement of the draw solutes to the feed solution and charged species of the feed solution towards the draw solution which results in high reverse salt flux and low rejection of the ions present in the feed solution, respectively. The influence of charged draw solutes on the rejection by the selective layer is expected to be higher in PRO mode (selective layer facing draw solution) due to direct exposure of the selective layer to the draw solution. This influence must be lower in FO mode (selective layer facing feed solution) due to dilutive ICP which results in a much-diluted draw solution present at the selective layer. Therefore, a charged solute can lead to lower rejection and higher reverse salt flux as compared with an uncharged solute depending on the operation mode. The use of charged draw solutes then can be favorable for treating non-ionic solutions while the uncharged draw solutes can be utilized for treating ionic wastewater solutions containing charged species such as e.g. charged micropollutants. Therefore, the draw solution for polyelectrolyte-based FO membranes should be chosen in accordance with the valency of the feed solution and the process orientation (FO or PRO mode).

In this study, to avoid defects from IP-coating and time-consuming post-treatment steps, we try to produce the selective layer during spinning in a single-step. This selective layer is produced by direct complexation of two PEs present in the spinning solutions. Due to the polyelectrolyte layer typically being in the nanofiltration (NF) separation range and using pure water as feed solution (uncharged solution), we limit ourselves to the use of a large and charged draw solution (TSC) in the FO and PRO experiments. The concept of using a single-step asymmetric NF hollow fiber membrane in the FO process has been already explored by Wang et al. [48]. To achieve the best performance of their NF membrane, they chose $MgCl_2$ as draw solution after showing higher rejection in pressure-driven (RO) mode as compared with other salts tested ($MgSO_4$, Na_2SO_4, NaCl). In another study, a single-step NF-like selective layer formation during support spinning was developed, involving cross-linking polyethylene imine (PEI) to the polyimide support [49,50]. More recently, single-step polyelectrolyte complex (PEC) hollow fibers with NF properties were prepared by using oppositely charged polyelectrolytes [51,52]. However, these PEC membranes were never intended for use in an FO process.

In this paper, the PEC selective layer made in a single-step process is investigated via measurements of the streaming potential, pure water permeance, MWCO, and scanning electron microscopy. We then determine the rejection ability of the PEC membrane towards different salts in a pressure-driven (RO) filtration process. Moreover, we assess our membrane rejection against TSC at four different concentrations to evaluate the influence of ionic strengths on PEC layer rejection. Our approach successfully shows that a defect-free, simple, and high-performance FO hollow fiber can be developed.

2. Experimental

2.1. Materials

Polyimide Matrimid® 5218 was purchased from Huntsman (USA). Trisodium citrate dehydrate (TSC) 98%, poly(4-styrenesulfonic acid) (PSS, Mw ~ 75,000 g·mol^{-1} 18 wt% solution), poly(diallyldimethylammonium chloride) (PDADMAC, Mw ~ 400,000–500,000 g·mol^{-1} 30 wt% solution), polyethylene glycol (PEG400, Mw ~ 400 g·mol^{-1}), glycerol 86–89% solution, and $MgCl_2$, Na_2SO_4, $MgSO_4$, and NaCl were acquired from Sigma (Germany). All polyethylene glycols used for the MWCO determination were obtained from Sigma (Germany). 1-methyl-2-pyrrolidinone (NMP; 99%) was supplied by Acros Organics (the Netherlands). Sulfonated polyethersulfone (SPESU) (GM0559/111) was obtained from BASF (Germany). All chemicals

except PSS (see section 2.2.) were used as received without further modification.

2.2. Preparation of PEC Hollow-Fiber membranes

Two different types of hollow fibers – bare fibers and coated fibers – were prepared using a dry-jet wet spinning technique [26]. The polyimide (PI) used as base polymer was air-dried in an oven at 100 °C for 24 h prior to dope solution preparation. The 18 wt% PSS solution was completely dried in the drying oven at 100 °C for 24 h to obtain pure PSS. The dried PSS was ground for better mixing in the dope solution preparation. The polymer dope was prepared by mixing PI (16% w/w), SPESU (2% w/w), PSS (2% w/w), PEG400 (12% w/w) with NMP (68% w/w) in a bottle. The dope composition was based on the work of Dutczak et al. [49] and modified accordingly. A homogenous polymer solution was obtained after placing the bottle on a roller bench to allow overnight mixing. The solution was left in the polymer container of the spinning machine for 48 h at 65 °C for degassing prior to spinning the hollow fibers. The bore solutions were also prepared on the roller bench overnight and were left at room temperature for degassing. Table 1 provides more details on bore compositions and spinning conditions. The newly spun fibers were rinsed for 72 h in deionized water prior to being post-treated for 24 h with 20% w/w glycerol aqueous solution to prevent pore collapse during drying. The fibers then were allowed to air-dry at ambient temperature for 24 h until further use.

2.3. Module preparation

The fibers were potted in a 16-cm-long module housing (potting resin: RenCast® FC 52/53 Isocyanate / FC 52 Polyol). These modules contained 38 fibers with an effective length of 10.7 cm for every single fiber; see Fig. 1.

2.4. Membrane characterization

2.4.1. Scanning electron microscopy

The hollow fibers were fractured in liquid nitrogen to prepare samples for cross-section imaging. For inner surface sample preparation, the fibers were cut in half diagonally with a sharp razor blade. All samples were mounted on designated holders and stored in a vacuum oven at 30 °C. The samples were sputter-coated with a 10-nm chromium layer (Q150T ES sputter coater; Quorum Technologies, UK) before microscopy. The cross-section and surface images were obtained with a JEOL JSM-6010LA scanning electron microscope.

2.4.2. Zeta potential and Debye length determinations

The apparent zeta potential of the fibers was determined with a SurPASS electrokinetic analyzer (Anton Paar, Austria) at different pH values ranging from 3 to 11, using 5 mM KCl as the electrolyte solution. For this purpose, three fibers from each batch were selected and potted individually in a 7-cm-long tubing. The streaming potential was determined by flowing the electrolyte solution inside the lumen of the fibers [28], measured six times at each pH point, and then averaged. The pH was adjusted by automatic titration with 0.1 M HCl and 0.1 M NaOH. We calculated the zeta potential with Eq. (1).

Table 1
Spinning parameters for the preparation of Bare and PEC hollow fibers.

Polymer dope: 16% (w/w) PI, 2% (w/w) SPESU, 2% (w/w) PSS, 12% (w/w) PEG400, 68% (w/w) NMP					
Coagulant bath: Tap water at 65 °C					
Fibers	Bore liquid composition (%) (w/w)				
	NMP	Glycerol	H_2O	PEG400*	PDADMAC
Bare	50	25	25	–	–
PEC	–	20	45	30	5
Spinning condition	Dope temperature		65 °C		
	Dope flow rate		3.9 mL·min^{-1}		
	Bore temperature		Ambient		
	Bore flow rate		3 mL·min^{-1}		
	Take-up speed		2.4 m·min^{-1}		
	Air gap		10 cm		
	Humidity		31%		
	Temperature		22.5 °C		

* NMP was replaced with PEG400 in the bore used for PEC fibers to ensure PDADMAC solubility.

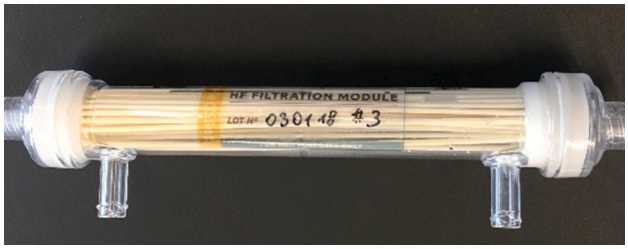

Fig. 1. The module containing 38 fibers with a total membrane area of 112 cm^2.

$$\zeta = \frac{dI}{dP}\frac{\eta}{\varepsilon\varepsilon_0}\frac{L_s}{A_s} \quad (1)$$

In this equation, ζ is the apparent zeta potential (V), I is the streaming current (A), P is the pressure (Pa), η is the dynamic viscosity of the electrolyte solution (Pa·s), ε is the dielectric permittivity of the water, ε_0 is the dielectric permittivity in vacuum (F·m^{-1}), L_s is the channel length (m), and A_s is the cross-sectional of the streaming channel (m^2).

2.4.3. Pure water permeance measurements

The pure water permeance (PWP) (L·m^{-2}·h^{-1}·bar^{-1}) of the fibers was derived from measurements in a dead-end, inside-out mode at 2 bars (using compressed nitrogen), using Eq. (2).

$$PWP = \frac{V}{tA\Delta P} \quad (2)$$

where V is the volume of collected permeate (L), t is the collecting time (h), A is the membrane's inner surface area (m^2), and ΔP is the pressure difference between the feed side and the permeate side of the membrane (bar).

2.4.4. Salt rejection determinations

The PEC membrane's rejection of several salts (NaCl, $MgCl_2$, $MgSO_4$, Na_2SO_4, TSC; 500 mg·L^{-1} aqueous solution; pH 5.8) was determined in a cross-flow filtration system at a transmembrane pressure of 1 bar. The cross-flow velocity in the module was set to 0.76 m·s^{-1}. For TSC, we determined the rejection ability of the PEC fiber at different concentrations of TSC. The rejection was calculated with Eq. (3) by measuring the conductivity of the feed solution and of the collected permeate.

$$R = \frac{(\sigma_f - \sigma_p)}{\sigma_f} \times 100\% \quad (3)$$

In this equation, R is the salt rejection percentage (%), σ_f is the conductivity of the feed solution (μS·cm^{-1}), and σ_p is the conductivity of the permeate solution (μS·cm^{-1}).

The water permeance (A) (L·m^{-2}·h^{-1}·bar^{-1}) was determined as follows:

$$A = \frac{V}{tA(\Delta P - \Delta\pi)} \quad (4)$$

Here, V is the permeate volume (L), t is the collection time (h), A is the effective area of the membrane (m^2), ΔP is the transmembrane pressure difference (bar), and $\Delta\pi$ is the osmotic pressure difference between the feed and permeate.

The salt permeance (B) was determined after Yip et al. [53], with a mass transfer coefficient (K) ($L{\cdot}m^{-2}{\cdot}h^{-1}$) according to the Lévêque correlation for a fully developed laminar velocity profile in a tube [54].

$$B = J_w\left(\frac{1-R}{R}\right)\exp\left(-\frac{J_w}{K}\right) \quad (5)$$

2.4.5. Molecular weight cut-off estimation

Two solutions containing a mixture of different polyethylene glycol (PEG) molecules were used to determine the molecular weight cut-off (MWCO). The first mixture contained PEGs with a molecular range of 62–2,000 $g{\cdot}mol^{-1}$, while the second had PEGs with a molecular range of 4,000–35,000 $g{\cdot}mol^{-1}$. The solutions were filtered in an inside-out configuration at the TMP of 2 bars and a cross-flow of 2 $L{\cdot}h^{-1}$. The MWCO of a membrane is defined as the molecular weight at which a molecule is rejected for 90%. Gel permeation chromatography (GPC) was utilized to define the MWCO after analyzing the feed and permeate samples of the filtration test. The GPC was equipped with a size exclusion column (Agilent 1200/1260 Infinity GPC/SEC series). The samples were fed at 1 $mL{\cdot}min^{-1}$ to column of 1000 Å, 10 μm and a column of 30 Å, 10 μm. The concentrations of the different PEGs were determined via refractive index measurements.

2.4.6. Osmotic performance measurements

The osmotic performance of the fibers was evaluated by orienting the membrane in both FO mode (selective layer facing the feed) and PRO mode (selective layer facing the draw). The tests were conducted in a counter-current configuration using either 0.5 M or 1 M TSC as draw solution with a cross-flow of 4.8 $L{\cdot}h^{-1}$ per module for both FS and DS (corresponding to 5.8 $cm{\cdot}s^{-1}$ for the lumen side). The experiment was carried out for 1 h; the water flux (J_w) was determined by measuring the water transferred from the feed solution to the draw solution per unit of (membrane) area per unit of time. The reverse salt flux (J_s) was determined by measuring the feed solution's conductivity per unit of (membrane) area per unit of time. The quantity of solute that passed to the feed side was measured with the aid of a calibration curve.

The structural parameter (S) was estimated by a fitting method (simplified by neglecting ECP) [55,56] using Eq. (6) for FO mode,

$$S = \frac{D}{J_w}\ln\frac{B + A\pi_D}{B + J_w + A\pi_F} \quad (6)$$

and using Eq. (7) for PRO mode:

$$S = \frac{D}{J_w}\ln\frac{B - J_w + A\pi_D}{B + A\pi_F} \quad (7)$$

Here, J_w ($L{\cdot}m^{-2}{\cdot}h^{-1}$) is the osmotic water flow, D ($m^2{\cdot}h^{-1}$) is the solute diffusivity (1.7×10^{-6} $m^2{\cdot}h^{-1}$ for TSC [57]), π_D (bar) is the osmotic pressure of the draw solution and π_F (bar) is the osmotic pressure of the feed solution.

3. Results and discussion

3.1. The molecular weight cut-off and morphology of the fibers

The molecular weight cut-off the PEC fibers was determined as 2.0 ± 0.30 kDa which categorizes the membranes in the nanofiltration regime. Fig. 2 displays SEM images showing the morphology the PEC fiber, while the morphology of the Bare fiber can be found in the supporting document. The inner diameter of the PEC fibers was 880 ± 40 μm and its wall thickness was 160 ± 10 μm.

The presence of a polyelectrolyte complex (PEC) layer is evident in both the cross-sectional (Fig. 2 P-c) and surface images (Fig. 2 P-d). The observed roughness of the lumen side of the PEC fibers corresponds with the roughness of thick polyelectrolyte complexes reported elsewhere [51].

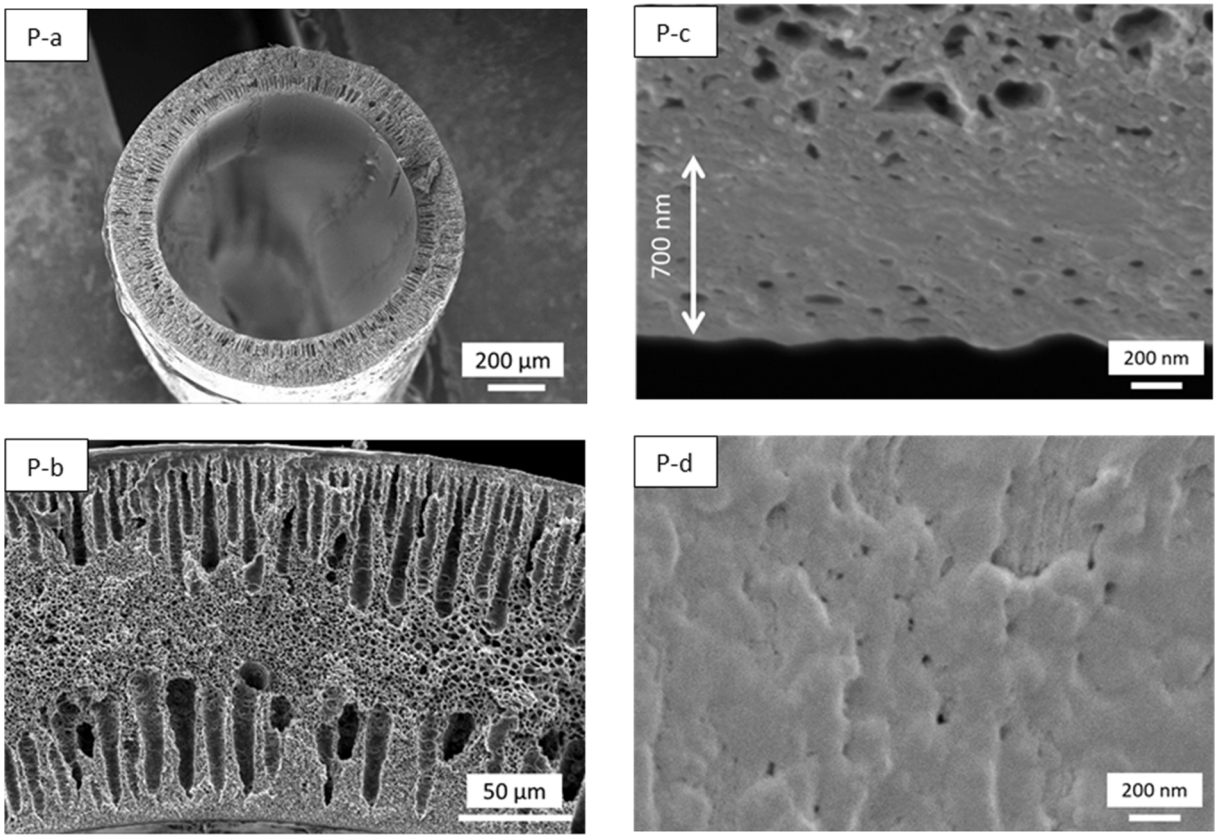

Fig. 2. SEM images PEC (P) fibers: a) cross section, b) magnified cross section, c) cross section of inner (selective) layer, d) lumen (inner) surface.

3.2. The zeta potential of the inner surface

The zeta potential was determined on the inner surface of the fibers in the pH range of 3–11 to assess the surface charge (Fig. 3). Differences in the zeta potential give a clear indication of a successful coating of the inner surface of the fibers. Furthermore, examining the zeta potential of the fibers helps to elucidate the different solute rejection mechanisms, especially for membranes with a dense selective layer [58]. Whereas the zeta potential of the bare fiber was in the range of −10 to −45 mV, the PEC fiber showed a partly (depending on pH) positively charged surface, as indicated by its zeta potential range of +10 to −30 mV. The PEC fiber has its isoelectric point at pH around 4.5 and exhibits a negatively-charged surface above pH 4.5. This zeta potential profile does not completely reflect the zeta-potential expected from PDADMAC. As PDADMAC is a strong polyelectrolyte, its charge is relatively independent of pH in the range we are measuring [59]. The pH dependence observed in our experiments shows that the polyimide (PI), which does have a pH-dependent zeta potential, contributes to the observed final zeta potential of the PEC membrane. This is in contrast with post-modified Layer-by-Layer membranes, of which the zeta potential is mostly determined by the final polyelectrolyte coated [35]. The notable contribution of the PI to the zeta potential suggests that the PEC is an intrinsic part of the support as a result of the single-step preparation method, which indicates that the selective layer is robust.

3.3. Salt rejection

The bare fibers had a pure water permeance (PWP) of 55 ± 14 ($L{\cdot}m^{-2}{\cdot}h^{-1}{\cdot}bar^{-1}$), while the PEC fibers had a substantially lower PWP of 2 ± 0.6 ($L{\cdot}m^{-2}{\cdot}h^{-1}{\cdot}bar^{-1}$). In addition to the zeta potential and the SEM images, this lower PWP also clearly indicates that a dense PEC layer was present. The rejection of the PEC fiber was determined by filtering different solutes in water. This was done to verify the effectiveness of the selective layer as well as to find a suitable solute for use as draw solution. The solute selection was made such that it covered different molecular weights and valencies. In nanofiltration, typically three main rejection mechanisms are considered: Donnan exclusion, dielectric exclusion, and size exclusion [60–62]. An important aspect in all these rejection mechanisms is that the solute concentration substantially influences its rejection. With increasing salt concentrations, lower solute rejection is to be expected, e.g. due to charge screening or Debye length reductions of the pores [63–65] as well as swelling of the PEC layer [46]. It is therefore important to consider rejection of the draw solute at different concentrations. Especially in PRO mode, high solute concentrations occur at the membrane surface due to concentrative ICP, whereas lower solute concentrations are present at the selective layer in FO mode because of dilutive ICP.

Fig. 4 shows the salt rejection of the PEC fibers at a transmembrane pressure of 1 bar and a pH of 5.8. The bare hollow fiber demonstrated no rejection of any of the salts in our experiments (results not shown). The PEC hollow fiber membrane had a better ability to reject multivalent anions than multivalent cations, which can be attributed to Donnan and dielectric exclusion. This finding agrees with the zeta potential results, which indicated that the PEC fiber had a negatively charged surface at pH values above 5.

The PEC membrane showed the lowest rejection towards NaCl (25 ± 13%) which is attributed to the nature of the PE selective layers as discussed before. A similar trend was observed for the PEC membrane produced from PSS/PDADMAC where the NF-like PEC membrane showed the lowest rejection for NaCl (around 30% at 2 bar) as compared with the other salts tested [51]. The solute rejection of our PEC membrane increases for different salts showing the highest rejection of 97 ± 2% for TSC. It is clear that despite being a leaky membrane for small salts such as NaCl, it is highly selective (tight) towards salts such as TSC. Therefore, these NF results indicated that TSC is very suitable to be used as draw solute in FO processes using our PEC membrane.

Furthermore, the effect of the TSC concentration on its rejection in pressure-driven mode was studied (Fig. 5), as the difference in concentration between the membranes pores and the bulk solution affects the membrane's selectivity substantially [66]. The ion rejection of nanofiltration membranes like our PEC membrane decreases with increasing the salt concentration as electrostatic interactions are involved in the rejection mechanisms [67]. In addition, polyelectrolyte-based selective layers are prone to swelling (hydration) under high ionic strengths resulting in lower rejection [46]. As expected, ion rejection decreased with increasing TSC concentration. The PEC fibers showed very high rejection for a 0.005 M TSC solution (97 ± 1%), while this dropped to 28 ± 6% for a concentration of 0.05 M TSC and to below 10% for 0.5 M and 1 M.

3.4. Osmotic performance

As mentioned in Section 3.3, we selected TSC as draw solution because of its very high rejection in the pressure-driven mode and due to the fact that we use pure water (uncharged solution) as feed solution for our experiments. TSC has been already used as draw solution for assessing the FO performance of polyelectrolyte-based membrane [42]. The PEC fiber membrane was evaluated for its osmotic performance in FO and PRO mode, with 0.5 M and 1 M TSC (Fig. 6).

In FO mode, the PEC membrane possessed a high rejection towards the draw solute, having reverse fluxes as low as 1.7 ± 0.6 and 2.1 ± 0.7 ($g{\cdot}m^{-2}{\cdot}h^{-1}$) when using 0.5 M and 1 M TSC draw solutions, respectively.

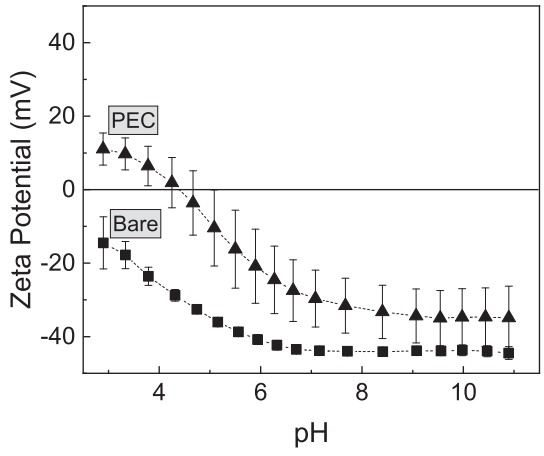

Fig. 3. Zeta potential as function of pH for bare and PEC fibers (bars represent the standard deviation of 3 fibers, with 6 measurements for each).

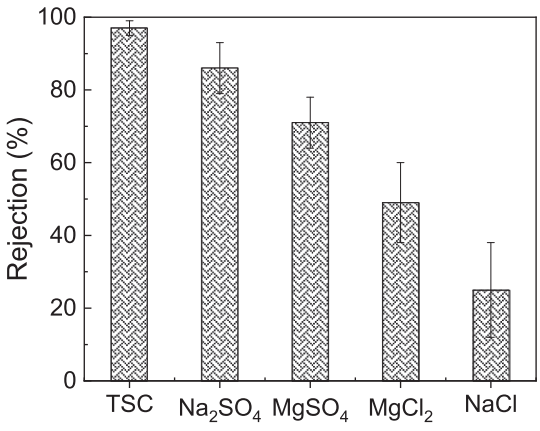

Fig. 4. Salt rejection ability of PEC fibers at 1 bar, 500 $mg{\cdot}L^{-1}$ aqueous solutions at pH 5.8, error bars represent the standard deviation based on three independent replicates (n = 3).

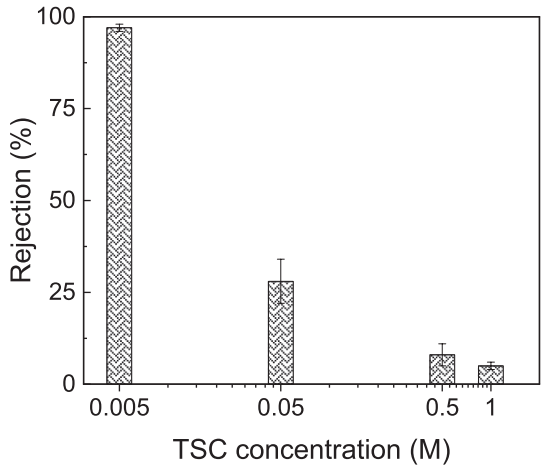

Fig. 5. The measured rejection at four different TSC concentrations, bars represent the standard deviation based on three independent replicates (n = 3).

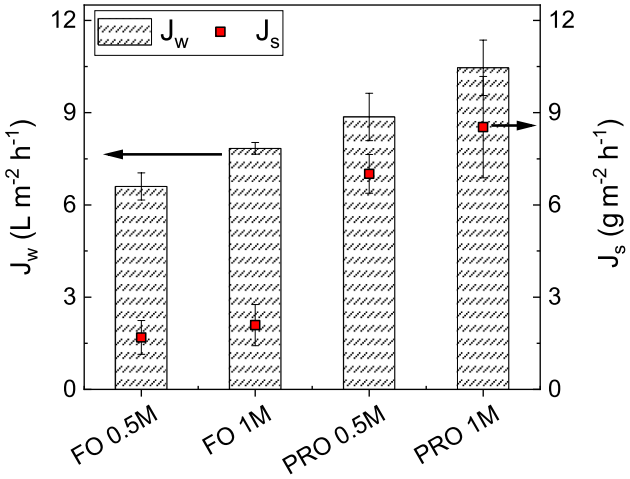

Fig. 6. Osmotic performance of PEC hollow-fiber membranes in FO and PRO modes, with 0.5 M and 1 M trisodium citrate (TSC) as draw solutions, n = 3.

In principle, membrane supports in FO mode display a resistance toward draw solute transport back to the separation, which leads to dilutive ICP. This results in a diluted draw solution present at the selective layer; hence a lower driving force achieved than in PRO mode [68] and consequently a lower water flux is achieved. In addition, the diluted charged draw solution has a positive impact on the rejection of the PEC layer, as discussed before, resulting in better rejection of the draw solutes; hence leading to a lower reverse salt flux.

In PRO mode, higher water fluxes were obtained for both draw concentrations than in FO mode (Fig. 6). The reason is that in PRO mode, the support experiences concentrative ICP instead of dilutive ICP [9,69]. Consequently, a greater concentration difference (osmotic pressure gradient) exists at the selective layer, leading to a greater water flux. However, also a significantly greater reverse salt flux was seen in PRO mode at both draw concentrations. The reason for this is that the PEC selective layer shows less ion rejection in highly concentrated solutions, such as the used 0.5 M and 1 M draw solutions. The substantial difference in TSC rejection at higher concentrations explains the high reverse salt flux observed in PRO mode.

The FO results also show that after doubling the draw solution concentration from 0.5 M to 1 M TSC, the water flux only increased slightly. This finding is in agreement with the S parameter results, showing that the support properties remained constant when the driving force was doubled. In other words, this means that our FO membrane is already at its highest capacity at a draw solute concentration of 0.5 M TSC; beyond this point, increasing the concentration no longer results in a substantial increase in water flux. This is an inherent disadvantage of FO, caused by the ICP, which is more severe at higher draw solution concentrations [68]. This results in a higher mass transport limitation within the porous support and subsequently only a low increase in water flux is gained at higher draw solute concentrations [70]. A similar trend was also observed in the study of Wei et al. [57], in which the FO water flux increased more significantly in the osmotic pressure range of 0 to 20 bar (~0–0.3 M TSC) than in the range of 20 to 70 bar (~0.3–1.2 M TSC), with TSC as draw solute.

The propensity to cause ICP can be determined by a term called the structural parameter (Eqs. (6) and (7)). The structural parameter can be seen as the effective wall thickness that solutes need to cross to reach the selective layer. Due to the tortuosity and the porosity of the support, the calculated S parameter (effective wall thickness) is typically greater than the support's actual wall thickness. This was also observed for our PEC membranes, for which structural parameters of S = 0.67 ± 0.08 (mm) and S = 0.67 ± 0.03 (mm) were determined with 0.5 M and 1 M TSC, respectively. These S parameters are acceptable, but lower values have been reported in the literature [71–73]. Reducing the S parameter could be accomplished by improving the support by, for instance, making the support more porous or thinner.

Our results clearly indicate that a polyelectrolyte-based membrane is especially challenging for PRO processes with charged solutes as draw solution because the solute retention suffers severely from concentrative ICP. Yet, we also show that polyelectrolyte-based membranes are much more viable in FO mode, exhibiting dilutive ICP and thus resulting in lower reversed salt fluxes. Nonetheless, we must emphasize that also FO processes are expected to be challenging when the most common draw solute, NaCl, will be used. This is due to the typical low rejection of these monovalent salts for polyelectrolyte-based membranes. However, we also show that when choosing a proper draw solution (e.g. TSC) and the proper orientation (FO mode), the PEC membrane can yield good FO performance. Additional useful experiments could include the evaluation of the performance of a PEC membrane using an uncharged draw solute such as e.g. sucrose.

4. Conclusions

In this study, a PEC-coated hollow-fiber membrane for the use in FO was prepared in a single-step process to avoid the challenging and time-consuming separate step of coating the supports. This membrane is based on polyimide as dope polymer. PDADMAC and PSS polyelectrolytes were used for the formation of the PEC selective layer. Using 1 M TSC as a draw solution, the created membrane has osmotic water fluxes of ($J_w = 7.8 \pm 0.2$ L·m^{-2}·h^{-1}, $J_s = 2.1 \pm 0.7$ g·m^{-2}·h^{-1}) and ($J_w = 10.5 \pm 1$ L·m^{-2}·h^{-1}, $J_s = 9 \pm 2$ g·m^{-2}·h^{-1}) in FO and PRO mode, respectively. Our results also show that the choice of draw solute and process orientation are very crucial in osmotic driven processes, especially for these membranes with relatively open polyelectrolyte-based selective layers. While in PRO mode the membrane selectivity declines due to concentrative concentration polarization, in FO mode the selectivity is still maintained. Our results show that most polyelectrolyte-based membranes can be potential candidate for FO applications especially, provided that larger draw solutes are used. However, to be able to use the most common draw solution (NaCl) and benefit from its advantages such as e.g. low price, and availability, we note that post modification of the polyelectrolytes or conventional IP based layer are more promising methods to yield highly selective layers that are needed for this draw solution.

CRediT authorship contribution statement

M. Mohammadifakhr: Conceptualization, Data curation, Investigation, Methodology, Writing - original draft. **J. de Grooth:**

Conceptualization, Project administration, Supervision, Writing - review & editing, Funding acquisition. **K. Trzaskus:** Conceptualization, Supervision. **H.D.W. Roesink:** Conceptualization, Supervision, Writing - review & editing, Funding acquisition. **A.J.B. Kemperman:** Conceptualization, Project administration, Supervision, Writing - review & editing.

Declaration of Competing Interest

The authors declare that they have no known competing financial interests or personal relationships that could have appeared to influence the work reported in this paper.

Acknowledgements

The authors are grateful to Aquaporin A/S (Lyngby, Denmark) and the TKI HTSM, through the 'Top Technology Twente' UT Impulse program for financial support.

Appendix A. Supplementary data

Supplementary data to this article can be found online at https://doi.org/10.1016/j.seppur.2021.118430.

References

[1] C.D. Moody, J.O. Kessler, Forward osmosis extractors, Desalination 18 (1976) 283–295, https://doi.org/10.1016/S0011-9164(00)84118-1.
[2] R.E. Kravath, J.A. Davis, Desalination of sea water by direct osmosis, Desalination 16 (1975) 151–155, https://doi.org/10.1016/S0011-9164(00)82089-5.
[3] K.B. Petrotos, H.N. Lazarides, Osmotic concentration of liquid foods, J. Food Eng. 49 (2001) 201–206, https://doi.org/10.1016/S0260-8774(00)00222-3.
[4] E.M. Garcia-Castello, J.R. McCutcheon, M. Elimelech, Performance evaluation of sucrose concentration using forward osmosis, J. Memb. Sci. 338 (2009) 61–66, https://doi.org/10.1016/j.memsci.2009.04.011.
[5] B. Jiao, A. Cassano, E. Drioli, Recent advances on membrane processes for the concentration of fruit juices: a review, J. Food Eng. 63 (2004) 303–324, https://doi.org/10.1016/j.jfoodeng.2003.08.003.
[6] K. Lutchmiah, A.R.D. Verliefde, K. Roest, L.C. Rietveld, E.R. Cornelissen, Forward osmosis for application in wastewater treatment: A review, Water Res. 58 (2014) 179–197, https://doi.org/10.1016/j.watres.2014.03.045.
[7] C.Y. Tang, Q. She, W.C.L. Lay, R. Wang, A.G. Fane, Coupled effects of internal concentration polarization and fouling on flux behavior of forward osmosis membranes during humic acid filtration, J. Memb. Sci. 354 (2010) 123–133, https://doi.org/10.1016/j.memsci.2010.02.059.
[8] A. Tiraferri, N.Y. Yip, W.A. Phillip, J.D. Schiffman, M. Elimelech, Relating performance of thin-film composite forward osmosis membranes to support layer formation and structure, J. Memb. Sci. 367 (2011) 340–352, https://doi.org/10.1016/j.memsci.2010.11.014.
[9] G.T. Gray, J.R. McCutcheon, M. Elimelech, Internal concentration polarization in forward osmosis: role of membrane orientation, Desalination 197 (2006) 1–8, https://doi.org/10.1016/j.desal.2006.02.003.
[10] D. Zhao, S. Chen, P. Wang, Q. Zhao, X. Lu, A Dendrimer-Based Forward Osmosis Draw Solute for Seawater Desalination, Ind. Eng. Chem. Res. 53 (2014) 16170–16175, https://doi.org/10.1021/ie5031997.
[11] J.R. McCutcheon, M. Elimelech, Influence of concentrative and dilutive internal concentration polarization on flux behavior in forward osmosis, J. Memb. Sci. 284 (2006) 237–247, https://doi.org/10.1016/j.memsci.2006.07.049.
[12] A. Achilli, T.Y. Cath, A.E. Childress, Selection of inorganic-based draw solutions for forward osmosis applications, J. Memb. Sci. 364 (2010) 233–241, https://doi.org/10.1016/j.memsci.2010.08.010.
[13] Q. She, X. Jin, C.Y. Tang, Osmotic power production from salinity gradient resource by pressure retarded osmosis: Effects of operating conditions and reverse solute diffusion, J. Memb. Sci. 401–402 (2012) 262–273, https://doi.org/10.1016/j.memsci.2012.02.014.
[14] G. Blandin, A.R.D. Verliefde, C.Y. Tang, A.E. Childress, P. Le-Clech, Validation of assisted forward osmosis (AFO) process: Impact of hydraulic pressure, J. Memb. Sci. 447 (2013) 1–11, https://doi.org/10.1016/j.memsci.2013.06.002.
[15] R. Wang, L. Shi, C.Y. Tang, S. Chou, C. Qiu, A.G. Fane, Characterization of novel forward osmosis hollow fiber membranes, J. Memb. Sci. 355 (2010) 158–167, https://doi.org/10.1016/j.memsci.2010.03.017.
[16] X. Liu, M.L. Bruening, Size-Selective Transport of Uncharged Solutes through Multilayer Polyelectrolyte Membranes, Chem. Mater. 16 (2004) 351–357, https://doi.org/10.1021/cm034559k.
[17] G. Han, S. Zhang, X. Li, N. Widjojo, T.-S. Chung, Thin film composite forward osmosis membranes based on polydopamine modified polysulfone substrates with enhancements in both water flux and salt rejection, Chem. Eng. Sci. 80 (2012) 219–231, https://doi.org/10.1016/j.ces.2012.05.033.
[18] J.E. Cadotte, L.T. Rozelle, In-situ formed condensation polymers for reverse osmosis membranes, OSW PB-Rep (1972).
[19] J.E. Cadotte, R.J. Petersen, R.E. Larson, E.E. Erickson, A new thin-film composite seawater reverse osmosis membrane, Desalination 32 (1980) 25–31, https://doi.org/10.1016/S0011-9164(00)86003-8.
[20] J.E. Cadotte, Interfacially synthesized reverse osmosis membrane, US Patent 4,277,344, (1981).
[21] F. Foglia, S. Karan, M. Nania, Z. Jiang, A.E. Porter, R. Barker, A.G. Livingston, J. T. Cabral, Neutron Reflectivity and Performance of Polyamide Nanofilms for Water Desalination, Adv. Funct. Mater. 27 (2017) 1701738, https://doi.org/10.1002/adfm.201701738.
[22] A.K. Ghosh, E.M.V. Hoek, Impacts of support membrane structure and chemistry on polyamide-polysulfone interfacial composite membranes, J. Memb. Sci. 336 (2009) 140–148, https://doi.org/10.1016/j.memsci.2009.03.024.
[23] Q. Zhang, Z. Zhang, L. Dai, H. Wang, S. Li, S. Zhang, Novel insights into the interplay between support and active layer in the thin fi lm composite polyamide membranes, J. Memb. Sci. 537 (2017) 372–383, https://doi.org/10.1016/j.memsci.2017.05.033.
[24] C.R. Bartels, A surface science investigation of composite membranes, J. Memb. Sci. 45 (1989) 225–245, https://doi.org/10.1016/S0376-7388(00)80516-5.
[25] F.J. Yang, D.L. Yang, S.H. Zhang, X.G. Jian, Synthesis of polypiperazine-amide thin-film membrane on PPESK hollow fiber UF membrane, Chinese Chem. Lett. 18 (2007) 966–968, https://doi.org/10.1016/j.cclet.2007.05.047.
[26] S.G. Li, G.H. Koops, M.H.V. Mulder, T. van den Boomgaard, C.A. Smolders, Wet spinning of integrally skinned hollow fiber membranes by a modified dual-bath coagulation method using a triple orifice spinneret, J. Memb. Sci. (1994), https://doi.org/10.1016/0376-7388(94)00076-X.
[27] H. Futselaar, H. Schonewille, W. van der Meer, Direct capillary nanofiltration for surface water, Desalination 157 (2003) 135–136, https://doi.org/10.1016/S0011-9164(03)00392-8.
[28] J. de Grooth, B. Haakmeester, C. Wever, J. Potreck, W.M. de Vos, K. Nijmeijer, Long term physical and chemical stability of polyelectrolyte multilayer membranes, J. Memb. Sci. 489 (2015) 153–159, https://doi.org/10.1016/j.memsci.2015.04.031.
[29] Y. Cui, H. Wang, H. Wang, T.-S. Chung, Micro-morphology and formation of layer-by-layer membranes and their performance in osmotically driven processes, Chem. Eng. Sci. 101 (2013) 13–26, https://doi.org/10.1016/j.ces.2013.06.011.
[30] C. Qiu, S. Qi, C.Y. Tang, Synthesis of high flux forward osmosis membranes by chemically crosslinked layer-by-layer polyelectrolytes, J. Memb. Sci. 381 (2011) 74–80, https://doi.org/10.1016/j.memsci.2011.07.013.
[31] P.H.H. Duong, J. Zuo, T.-S. Chung, Highly crosslinked layer-by-layer polyelectrolyte FO membranes: Understanding effects of salt concentration and deposition time on FO performance, J. Memb. Sci. 427 (2013) 411–421, https://doi.org/10.1016/j.memsci.2012.10.014.
[32] S. Qi, C.Q. Qiu, Y. Zhao, C.Y. Tang, Double-skinned forward osmosis membranes based on layer-by-layer assembly-FO performance and fouling behavior, J. Memb. Sci. 405–406 (2012) 20–29, https://doi.org/10.1016/j.memsci.2012.02.032.
[33] C. Liu, W. Fang, S. Chou, L. Shi, A.G. Fane, R. Wang, Fabrication of layer-by-layer assembled FO hollow fiber membranes and their performances using low concentration draw solutions, Desalination 308 (2013) 147–153, https://doi.org/10.1016/j.desal.2012.07.027.
[34] B. Tieke, F. van Ackern, L. Krasemann, A. Toutianoush, Ultrathin self-assembled polyelectrolyte multilayer membranes, Eur. Phys. J. E 5 (2001) 29–39, https://doi.org/10.1007/s101890170084.
[35] J. de Grooth, R. Oborný, J. Potreck, K. Nijmeijer, W.M. de Vos, The role of ionic strength and odd–even effects on the properties of polyelectrolyte multilayer nanofiltration membranes, J. Memb. Sci. 475 (2015) 311–319, https://doi.org/10.1016/j.memsci.2014.10.044.
[36] J. Park, J. Park, S.H. Kim, J. Cho, J. Bang, Desalination membranes from pH-controlled and thermally-crosslinked layer-by-layer assembled multilayers, J. Mater. Chem. 20 (2010) 2085–2091, https://doi.org/10.1039/B918921A.
[37] Q. Saren, C.Q. Qiu, C.Y. Tang, Synthesis and Characterization of Novel Forward Osmosis Membranes based on Layer-by-Layer Assembly, Environ. Sci. Technol. 45 (2011) 5201–5208, https://doi.org/10.1021/es200115w.
[38] L. Setiawan, R. Wang, K. Li, A.G. Fane, Fabrication of novel poly(amide-imide) forward osmosis hollow fiber membranes with a positively charged nanofiltration-like selective layer, J. Memb. Sci. 369 (2011) 196–205, https://doi.org/10.1016/j.memsci.2010.11.067.
[39] L. Setiawan, R. Wang, K. Li, A.G. Fane, Fabrication and characterization of forward osmosis hollow fiber membranes with antifouling NF-like selective layer, J. Memb. Sci. 394 (2012) 80–88, https://doi.org/10.1016/j.memsci.2011.12.026.
[40] X. Ding, Z. Liu, M. Hua, T. Kang, X. Li, Y. Zhang, Poly(ethylene glycol) crosslinked sulfonated polysulfone composite membranes for forward osmosis, J. Appl. Polym. Sci. 133 (2016) 1–8, https://doi.org/10.1002/app.43941.
[41] C.H. Tan, H.Y. Ng, Revised external and internal concentration polarization models to improve flux prediction in forward osmosis process, Desalination 309 (2013) 125–140, https://doi.org/10.1016/j.desal.2012.09.022.
[42] Y. Kang, S. Zheng, C. Finnerty, M.J. Lee, B. Mi, Regenerable Polyelectrolyte Membrane for Ultimate Fouling Control in Forward Osmosis, Environ. Sci. Technol. 51 (2017) 3242–3249, https://doi.org/10.1021/acs.est.6b05665.
[43] M. Hu, B. Mi, Layer-by-layer assembly of graphene oxide membranes via electrostatic interaction, J. Memb. Sci. 469 (2014) 80–87, https://doi.org/10.1016/j.memsci.2014.06.036.
[44] H. Salehi, M. Rastgar, A. Shakeri, Anti-fouling and high water permeable forward osmosis membrane fabricated via layer by layer assembly of chitosan/graphene

oxide, Appl. Surf. Sci. 413 (2017) 99–108, https://doi.org/10.1016/j.apsusc.2017.03.271.
[45] H.Y. Ng, W. Tang, W.S. Wong, Performance of Forward (Direct) Osmosis Process: Membrane Structure and Transport Phenomenon, Environ. Sci. Technol. 40 (2006) 2408–2413, https://doi.org/10.1021/es0519177.
[46] W. Cheng, C. Liu, T. Tong, R. Epsztein, M. Sun, R. Verduzco, J. Ma, M. Elimelech, Selective removal of divalent cations by polyelectrolyte multilayer nanofiltration membrane: Role of polyelectrolyte charge, ion size, and ionic strength, J. Memb. Sci. 559 (2018) 98–106, https://doi.org/10.1016/j.memsci.2018.04.052.
[47] G. Qiu, G.K.W. Wong, Y.-P. Ting, Electrostatic interaction governed solute transport in forward osmosis, Water Res. 173 (2020) 115590, https://doi.org/10.1016/j.watres.2020.115590.
[48] K.Y. Wang, T.-S. Chung, J.-J. Qin, Polybenzimidazole (PBI) nanofiltration hollow fiber membranes applied in forward osmosis process, 2007. https://doi.org/10.1016/j.memsci.2007.05.035.
[49] S.M. Dutczak, C.R. Tanardi, K.K. Kopeć, M. Wessling, D. Stamatialis, "Chemistry in a spinneret" to fabricate hollow fibers for organic solvent filtration, Sep. Purif. Technol. 86 (2012) 183–189, https://doi.org/10.1016/j.seppur.2011.11.003.
[50] K.K. Kopeć, S.M. Dutczak, M. Wessling, D.F. Stamatialis, Chemistry in a spinneret—On the interplay of crosslinking and phase inversion during spinning of novel hollow fiber membranes, J. Memb. Sci. 369 (2011) 308–318, https://doi.org/10.1016/j.memsci.2010.12.010.
[51] C.V. Gherasim, T. Luelf, H. Roth, M. Wessling, Dual-Charged Hollow Fiber Membranes for Low-Pressure Nanofiltration Based on Polyelectrolyte Complexes: One-Step Fabrication with Tailored Functionalities, ACS Appl. Mater. Interfaces (2016), https://doi.org/10.1021/acsami.6b05706.
[52] S. Emonds, H. Roth, M. Wessling, Chemistry in a spinneret – Formation of hollow fiber membranes with a cross-linked polyelectrolyte separation layer, J. Memb. Sci. 612 (2020), 118325, https://doi.org/10.1016/j.memsci.2020.118325.
[53] N.Y. Yip, A. Tiraferri, W.A. Phillip, J.D. Schiffman, M. Elimelech, High Performance Thin-Film Composite Forward Osmosis Membrane, Environ. Sci. Technol. 44 (2010) 3812–3818, https://doi.org/10.1021/es1002555.
[54] M. Mulder, Basic principles of membrane technology, Kluwer Academic Publishers, 1996.
[55] S. Loeb, L. Titelman, E. Korngold, J. Freiman, Effect of porous support fabric on osmosis through a Loeb-Sourirajan type asymmetric membrane, J. Memb. Sci. 129 (1997) 243–249, https://doi.org/10.1016/S0376-7388(96)00354-7.
[56] S. Lin, Mass transfer in forward osmosis with hollow fiber membranes, J. Memb. Sci. 514 (2016) 176–185, https://doi.org/10.1016/j.memsci.2016.04.053.
[57] J. Wei, C. Qiu, Y.N. Wang, R. Wang, C.Y. Tang, Comparison of NF-like and RO-like thin film composite osmotically-driven membranes-Implications for membrane selection and process optimization, J. Memb. Sci. 427 (2013) 460–471, https://doi.org/10.1016/j.memsci.2012.08.053.
[58] A.E. Childress, M. Elimelech, Relating Nanofiltration Membrane Performance to Membrane Charge (Electrokinetic) Characteristics, Environ. Sci. Technol. 34 (2000) 3710–3716, https://doi.org/10.1021/es0008620.
[59] L. Paltrinieri, K. Remmen, B. Müller, L. Chu, J. Köser, T. Wintgens, M. Wessling, L. C.P.M. de Smet, E.J.R. Sudhölter, Improved phosphoric acid recovery from sewage sludge ash using layer-by-layer modified membranes, J. Memb. Sci. 587 (2019) 117162, https://doi.org/10.1016/j.memsci.2019.06.002.
[60] D. Vezzani, S. Bandini, Donnan equilibrium and dielectric exclusion for characterization of nanofiltration membranes, Desalination 149 (2002) 477–483, https://doi.org/10.1016/S0011-9164(02)00784-1.
[61] A.E. Yaroshchuk, Non-steric mechanisms of nanofiltration: superposition of Donnan and dielectric exclusion, Sep. Purif. Technol. 22–23 (2001) 143–158, https://doi.org/10.1016/S1383-5866(00)00159-3.
[62] A. Szymczyk, P. Fievet, Investigating transport properties of nanofiltration membranes by means of a steric, electric and dielectric exclusion model, J. Memb. Sci. 252 (2005) 77–88, https://doi.org/10.1016/j.memsci.2004.12.002.
[63] A.E. Yaroshchuk, Dielectric exclusion of ions from membranes, Adv. Colloid Interface Sci. 85 (2000) 193–230, https://doi.org/10.1016/S0001-8686(99)00021-4.
[64] L.D. Nghiem, A.I. Schäfer, M. Elimelech, Role of electrostatic interactions in the retention of pharmaceutically active contaminants by a loose nanofiltration membrane, J. Memb. Sci. 286 (2006) 52–59, https://doi.org/10.1016/j.memsci.2006.09.011.
[65] C. Bartels, R. Franks, S. Rybar, M. Schierach, M. Wilf, The effect of feed ionic strength on salt passage through reverse osmosis membranes, Desalination 184 (2005) 185–195, https://doi.org/10.1016/j.desal.2005.04.032.
[66] O. Labban, C. Liu, T.H. Chong, J.H. Lienhard, Fundamentals of low-pressure nanofiltration: Membrane characterization, modeling, and understanding the multi-ionic interactions in water softening, J. Memb. Sci. 521 (2017) 18–32, https://doi.org/10.1016/j.memsci.2016.08.062.
[67] G. Hagmeyer, R. Gimbel, Modelling the salt rejection of nanofiltration membranes for ternary ion mixtures and for single salts at different pH values, Desalination 117 (1998) 247–256, https://doi.org/10.1016/S0011-9164(98)00109-X.
[68] Y. Xu, X. Peng, C.Y. Tang, Q.S. Fu, S. Nie, Effect of draw solution concentration and operating conditions on forward osmosis and pressure retarded osmosis performance in a spiral wound module, J. Memb. Sci. 348 (2010) 298–309, https://doi.org/10.1016/j.memsci.2009.11.013.
[69] E.R. Cornelissen, D. Harmsen, K.F. de Korte, C.J. Ruiken, J.J. Qin, H. Oo, L. P. Wessels, Membrane fouling and process performance of forward osmosis membranes on activated sludge, J. Memb. Sci. 319 (2008) 158–168, https://doi.org/10.1016/j.memsci.2008.03.048.
[70] Q. Wang, Z. Zhou, J. Li, Q. Tang, Y. Hu, Modeling and measurement of temperature and draw solution concentration induced water flux increment efficiencies in the forward osmosis membrane process, Desalination 452 (2019) 75–86, https://doi.org/10.1016/j.desal.2018.11.001.
[71] J. Ren, M.R. Chowdhury, J. Qi, L. Xia, B.D. Huey, J.R. McCutcheon, Relating osmotic performance of thin film composite hollow fiber membranes to support layer surface pore size, J. Memb. Sci. 540 (2017) 344–353, https://doi.org/10.1016/j.memsci.2017.06.024.
[72] M. Shibuya, M. Yasukawa, T. Takahashi, T. Miyoshi, M. Higa, H. Matsuyama, Effect of operating conditions on osmotic-driven membrane performances of cellulose triacetate forward osmosis hollow fiber membrane, Desalination 362 (2015) 34–42, https://doi.org/10.1016/j.desal.2015.01.031.
[73] J. Ren, J.R. McCutcheon, Polyacrylonitrile supported thin film composite hollow fiber membranes for forward osmosis, Desalination 372 (2015) 67–74, https://doi.org/10.1016/j.desal.2015.05.018.